

Morphology of prestellar cores in pressure confined filaments

S. Heigl,^{1,2}[★] M. Gritschneider,¹ A. Burkert,^{1,2}

¹*Universitäts-Sternwarte, Ludwig-Maximilians-Universität München, Scheinerstr. 1, 81679 Munich, Germany*

²*Max-Planck Institute for Extraterrestrial Physics, Giessenbachstr. 1, 85748 Garching, Germany*

Accepted XXX. Received YYY; in original form ZZZ

ABSTRACT

Observations of prestellar cores in star-forming filaments show two distinct morphologies. While molecular line measurements often show broad cores, submillimeter continuum observations predominantly display pinched cores compared to the bulk of the filament gas. In order to explain how different morphologies arise, we use the gravitational instability model where prestellar cores form by growing density perturbations. The radial extent at each position is set by the local line-mass. We show that the ratio of core radius to filament radius is determined by the initial line-mass of the filament. Additionally, the core morphology is independent of perturbation length scale and inclination, which makes it an ideal diagnostic for observations. Filaments with a line-mass of less than half its critical value should form broad cores, whereas filaments with more than half its critical line-mass value should form pinched cores. For filaments embedded in a constant background pressure, the dominant perturbation growth times significantly differ for low and high line-mass filaments. Therefore, we predict that only one population of cores is present if all filaments within a region begin with similar initial perturbations.

Key words: stars:formation – ISM:kinematics and dynamics – ISM:structure

1 INTRODUCTION

It has long been proposed that core formation in filaments is tied to some kind of fragmentation process (Schneider & Elmegreen 1979; Larson 1985). This connection has only been reinforced by observations of the *Herschel* Space Observatory (André et al. 2010; Könyves et al. 2010; Men’shchikov et al. 2010; Ward-Thompson et al. 2010; Arzoumanian et al. 2011, 2013; Kirk et al. 2013; André et al. 2014), which show that dense cores are contained in an ubiquitous filamentary structure in molecular clouds. As cores are the birth-site of stars (Benson & Myers 1989; Klessen et al. 1998; McKee & Ostriker 2007), it is essential to understand the process of core formation in order to develop a coherent model for stellar formation. Different models of core formation have been proposed, e.g. by the dissipation of turbulence (Padoan et al. 2001; Klessen et al. 2005) or by collapse of density enhancements due to intersecting filaments, so called “hubs” (Myers 2009). The complexity of core formation has increased with the observations of fibres (Hacar et al. 2013; Tafalla & Hacar 2015), trans- and subsonic velocity coherent substructures in filaments, again opening the possibility that cores form by

subsonic motions due to gravitational instabilities, potentially modified by magnetic fields either hindering core formation due to magnetic pressure (Nagasawa 1987; Gehman et al. 1996b; Fiege & Pudritz 2000) or facilitating core formation in a magnetically stabilized filament by ambipolar diffusion (Shu et al. 1987; Hosseinirad et al. 2017).

A possible indicator to validate this model is the comparison of observed cores with the analytical predictions of overdensities forming by gravitational instabilities. High dynamic range observations in the submillimeter continuum, for instance in the Taurus region, show very thin cores compared to the filament radius (Marsh et al. 2014). Contrarily, molecular line observations, which often only trace the dense gas, have mainly revealed cores which are broader than the filament (Hacar & Tafalla 2011; Hacar et al. 2013; Tafalla & Hacar 2015). Thus, the interpretation of core radius is complex and core morphology obviously depends on the tracer of observation.

Numerical predictions by Nagasawa (1987) showed that there are two regimes of the perturbation. One for low line-mass filaments, called deformation instability or “sausage” instability, where the forming cores bulge out and one for high line-mass, named compressional instability, where cores form by compression and thus pinch in. Both morphologies

[★] E-mail: heigl@usm.lmu.de

exist in simulations throughout the literature (Gehman et al. 1996a,b; Inutsuka & Miyama 1997; Fiege & Pudritz 2000). However, in order to determine the morphology of cores it is important to not only predict the radius evolution of the core itself, but also the radius evolution of the material making up the rest of the filament. For a growing perturbation, both evolve simultaneously. We expand on the picture by Nagasawa (1987) and show an analytical prediction for the evolution of the radius ratio.

2 BASIC CONCEPTS

In order to be able to calculate the radial extent of a filament, it is necessary to define the underlying density structure. The basic hydrostatic, isothermal model predicts a profile which drops off as r^{-4} (Stodólkiewicz 1963; Ostriker 1964). Observationally, filaments often show a shallower power law exponent of -1.6 to -2.5 at large radii (Arzoumanian et al. 2011; Palmeirim et al. 2013). Several processes can explain this difference: truncation of the filament radius in pressure equilibrium (Fischera & Martin 2012), magnetic fields (Fiege & Pudritz 2000), the equation of state (Gehman et al. 1996a; Toci & Galli 2015) or filaments formed by shock interaction (Federrath 2016). As the physical reason for the observed profile and how it would impact the radial stability is still unclear, we use the basic isothermal model. In this case the density goes as:

$$\rho(r) = \rho_c \left(1 + (r/H)^2\right)^{-2} \quad (1)$$

where r is the cylindrical radius and ρ_c is its central density. It has the radial scale height H given by

$$H^2 = \frac{2c_s^2}{\pi G \rho_c} \quad (2)$$

where c_s is the isothermal sound speed and G is the gravitational constant. Integrating the density profile to $r \rightarrow \infty$, one can calculate the critical line-mass, e.g. the line-mass at which a filament is marginally stable, of

$$\left(\frac{M}{L}\right)_{\text{crit}} = \frac{2c_s^2}{G}. \quad (3)$$

If the line-mass of a filament is above this value, there is no hydrostatic solution and the filament will collapse to a spindle. If the line-mass is below this value the filament will expand freely unless it is bound by an additional outside pressure (Nagasawa 1987). In this case, the filament follows the hydrostatic equilibrium profile until it extends to the radius where the internal pressure matches the external pressure. Following Fischera & Martin (2012), the integral of the density profile then is given by

$$\frac{M}{L} = \int_0^R 2\pi r \rho(r) dr = \left(\frac{M}{L}\right)_{\text{crit}} \left(1 + (H/R)^2\right)^{-1} \quad (4)$$

and the factor of line-mass to critical line-mass becomes

$$f_{\text{cyl}} = \left(\frac{M}{L}\right) / \left(\frac{M}{L}\right)_{\text{crit}} = \left(1 + (H/R)^2\right)^{-1}. \quad (5)$$

This allows us to derive the filament radius as

$$R = H \left(\frac{f_{\text{cyl}}}{1 - f_{\text{cyl}}}\right)^{1/2}. \quad (6)$$

For a fixed external pressure the scale height is not set by the central density but by the ambient pressure via the boundary density $\rho_b = p_{\text{ext}}/c_s^2$. It is related to the central density by

$$\rho_b = \rho_c \left(1 - f_{\text{cyl}}\right)^2 \quad (7)$$

and therefore the scale height adjusts as

$$H^2 = \frac{2c_s^2}{\pi G \rho_b} \left(1 - f_{\text{cyl}}\right)^2 = \frac{2c_s^4}{\pi G p_{\text{ext}}} \left(1 - f_{\text{cyl}}\right)^2. \quad (8)$$

Subsequently, the radius has a maximum at $f_{\text{cyl}} = 0.5$ and declines to zero as f_{cyl} approaches 0 or 1.

Linear perturbation analysis introduces a perturbation along the filament axis of the form

$$\rho(r, z, t) = \rho_0(r) + \rho_1(r, z, t) = \rho_0(r) + \epsilon \rho_0(r) \exp(ikz - i\omega t) \quad (9)$$

where z is the filament axis, $\omega = 2\pi/\tau$ is the perturbation growth rate with τ being the perturbation growth time, $k = 2\pi/\lambda$ is the wave vector with λ being the perturbation length scale and ϵ is the perturbation strength. This also leads to a perturbation in velocity, pressure and potential of the form:

$$q_1(r, z, t) \propto \exp(ikz - i\omega t). \quad (10)$$

Solving the mass and momentum conservation as well as Laplace's equation for the gravitational potential while second order terms are ignored, perturbations grow for values of k where the solution of the resulting dispersion relation $\omega^2(k)$ is smaller than zero. As the perturbation term of Equation 9 does not depend on radius, one can insert it into the definition of the line-mass Equation 4 and easily show that the line-mass

$$f_{\text{cyl}}(z, t) = f_0 (1 + \epsilon \exp(ikz - i\omega t)) \quad (11)$$

evolves analogous to the density with f_0 being the initial line-mass. Therefore, the filament radius now depends on the local line-mass at the position z .

3 CORE MORPHOLOGY

While Nagasawa (1987) already pointed out the two different core formation regimes, it is important to look at the dynamical evolution of both core and filament radius. As the radius has its maximum at half the critical line-mass, it can both grow or shrink for an increase or decrease in the local line-mass, depending on the initial line-mass. In low line-mass filaments, where the mean line-mass is below half the critical value, the growing core will first increase in radius. But as soon as its local line-mass exceeds a value of $f_{\text{cyl}} = 0.5$, the radius will decrease again. At the same time, in absence of accretion the core is fed by filament gas, thus reducing the line-mass and the radius of the rest of the filament. Contrarily, in a filament with initially high line-mass, where the mean line-mass is above half the critical value, the radius of the core decreases as it grows. As mass is accreted from the rest of the filament, the overall filament radius will at first increase but then also decrease as soon as the local line-mass is below a value of $f_{\text{cyl}} = 0.5$.

In order to determine the core morphology, one has to compare the radius R_{max} of the slice with the maximum line-mass to the radius R_{min} of the slice with the minimum line-mass. In a perturbed filament both evolve simultaneously

and determine how a core appears visually. If $R_{\max} > R_{\min}$ then the core will bulge out and will be broader than the rest of the filament gas. If $R_{\max} < R_{\min}$ the core will be narrower than the filament gas and will pinch in. The radii are given by the respective scale height and line-mass as shown in Equation 6. The ratio of the two is given by

$$\begin{aligned} R_{\max}/R_{\min} &= \frac{H_{\max} (f_{\max}/(1 - f_{\max}))^{1/2}}{H_{\min} (f_{\min}/(1 - f_{\min}))^{1/2}} = \\ &= \left(\frac{f_{\max}(1 - f_{\max})}{f_{\min}(1 - f_{\min})} \right)^{1/2} \end{aligned} \quad (12)$$

with

$$f_{\max} = f_0(1 + \epsilon \exp(\omega t)) = f_0 c_+ \quad (13)$$

and

$$f_{\min} = f_0(1 - \epsilon \exp(\omega t)) = f_0 c_- \quad (14)$$

Note that $c_- = 2 - c_+$. This means that

$$R_{\max}/R_{\min} = \left(\frac{c_+ - f_0 c_+^2}{c_- - f_0 c_-^2} \right)^{1/2}. \quad (15)$$

Setting this equation equal to 1, one can calculate the line-mass where cores stay exactly as broad as the filament to be half the critical line-mass. For smaller line-masses the ratio between the radii will at all times be larger than one and vice versa. This means that for a filament which has a line-mass of less than half the critical value, the decrease in radius of the core when it reaches a local line-mass greater than half the critical value will always be slower than the overall decrease of radius due to the loss of mass in the rest of the filament. Therefore, the core will bulge out at all times. The inverse is true for filaments with a line-mass above half the critical line-mass, where the core will always pinch in. This fact is illustrated in the top panel of Figure 1 where we show the evolution of the ratio between core to filament radius over time for a fixed initial central density of 10^4 cm^{-3} and an initial perturbation strength of 1%. As the central density and the external pressure are not independent of each other, a constant central density with a varying initial line-mass means that we vary the external pressure from $p_{\text{ext}}/k_B \sim 10^5 \text{ K cm}^{-3}$ for low line-masses to $p_{\text{ext}}/k_B \sim 10^3 \text{ K cm}^{-3}$ for high line-masses. The perturbation growth times are taken from Fischera & Martin (2012) where we assume the perturbation grows on the dominant wavelength. For the same initial density the growth time only depends weakly on the line-mass. Thus at the same point in time they have evolved by approximately the same factor. Note that although the radius in general does depend on the initial central density the ratio does not.

Interestingly, for filaments below half the critical line-mass the radius ratio does not depend much on the line-mass itself at a specific point in its evolution. As long as the cores have grown by about the same amount we do not expect a significant difference in core to filament radius. As f_{\min} goes to zero as soon as the core has accreted nearly all material, the radius ratio diverges to infinity. Note that Fischera & Martin (2012) predicted that cores could form an unstable Bonnor-Ebert sphere (Ebert 1955; Bonnor 1956) depending on the perturbation length. We do not include this effect in our analytical model but note that it can lead to the collapse

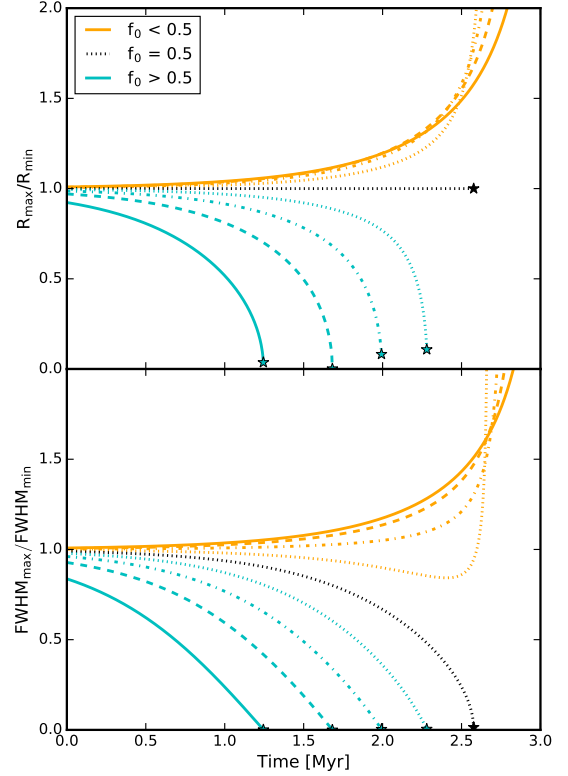


Figure 1. The top figure shows the analytical prediction of the ratio between the core radius (at the maximum central density) and filament radius (at the minimum central density) for a constant initial central density of $\rho_0 = 10^4 \text{ cm}^{-3}$, starting with a perturbation of 1%. The bottom figure shows the same for the FWHM. From top to bottom the curves show different values of the line-mass in values of f_0 , starting at 0.1 (solid orange) and incrementally increased by 0.1. The stars symbolize the time when the line-mass locally becomes supercritical and the core collapses. Note that the radius ratio of cores in low line-mass filaments diverges to infinity as all the gas of the filament is accreted.

of an initially broad core and therefore also could lead to a pinched, albeit protostellar core.

The evolution of cores is significantly different for filaments with a line-mass above half the critical value. They tend to evolve much faster than their counterparts in low line-mass filaments. As soon as they come close to the limit of hydrostatic equilibrium, their radius collapses away quite rapidly. This restricts their lifetime and the chance to actually observe pinched cores.

Additionally, we test our predictions by simulating the evolution of cores which start with a one per cent perturbation in filaments with a central density of 10^4 cm^{-3} and a line-mass of $f_{\text{cyl}} = 0.2$ and 0.8 in order to show the qualitative difference in morphology. We use the grid code RAMSES (Teyssier 2002) to set up boxes with the size of the respective dominant perturbation length with periodic boundary condition in the filament axis and open boundaries perpendicular to the filament. In order to test our prediction independent of accretion onto the filaments, they are embedded in a low-density warm medium in pressure equilibrium. The simulation set-up is similar to that of Heigl et al. (2016).

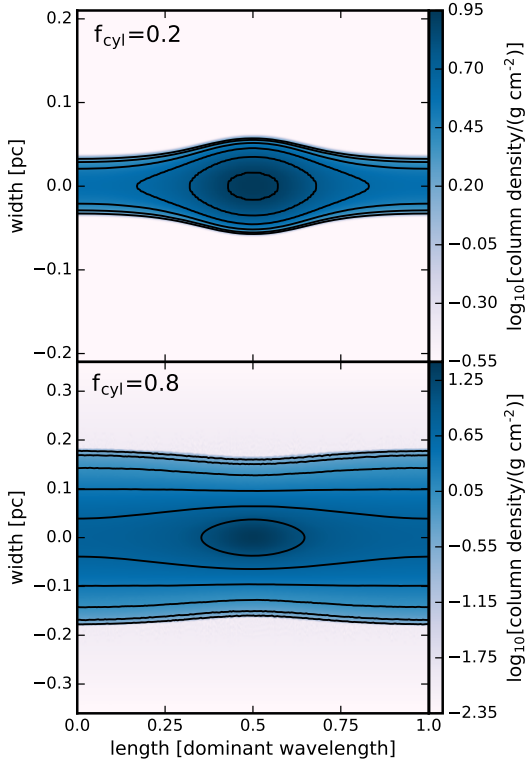


Figure 2. Column density plots of simulated cores forming in filaments with different line-masses. A low line-mass filament forms a broad core while a core forming in a high line-mass filament causes the radius to pinch.

Both results of the simulations are shown in projection in [Figure 2](#) at the same time, shortly before the high line-mass filament collapses. The difference in morphology is clearly visible. The core in the low line-mass filament is broader than the filament, whereas the core in the high line-mass filament causes the radius to decrease. We only see a divergence of the Ostriker profile at late times, where both cores profiles become softer and closer to the radial dependence of an isothermal sphere.

Therefore, our analysis provides observers with a useful tool to determine the line-mass a filament, independent of inclination and perturbation scale, by identifying the cores. If a core bulges out of the filament, the mean line-mass is below 0.5. If a core pinches inwards, the mean line-mass is above 0.5. A caveat of this method is the way the radius is determined in the observations. The filament width is often determined by measuring the full-width at half maximum (FWHM) of the radial profile. If the filament follows an Ostriker profile, the FWHM is not a perfect tracer of the radius and a correction term has to be taken into consideration. This correction was derived in [Fischera & Martin \(2012\)](#) and changes the analytical prediction of the radius ratio as shown in the bottom of [Figure 1](#). In general, using the FWHM will underestimate the core radius and therefore introduces a bias to lower radius ratios. This effect does not change the predicted curves significantly except for cores

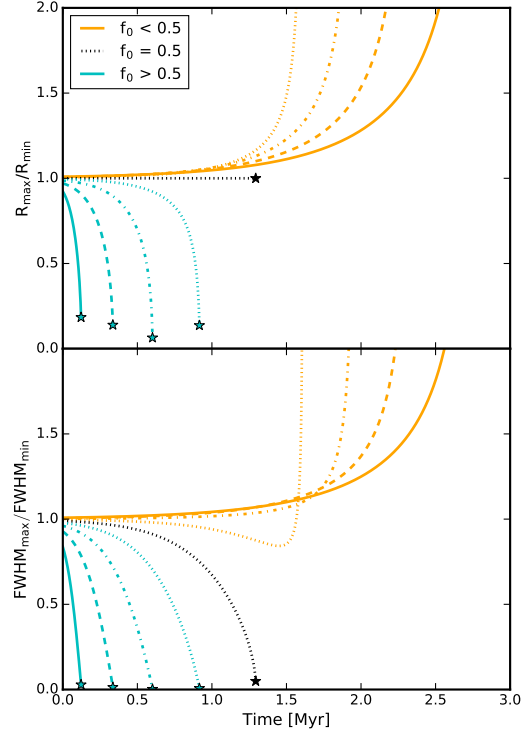


Figure 3. The same as in [Figure 1](#) but now for a constant external pressure of $p_{\text{ext}}/k_B = 10^5 \text{ K cm}^{-3}$. For varying central densities there is a broad spread in perturbation growth time. The line properties are the same as in [Figure 1](#). Starting at $f_0 = 0.1$ for the curve with the longest perturbation growth time (solid orange), f_0 increases incrementally by 0.1 going to faster perturbation growth times.

forming in filaments with $f_{\text{cyl}} = 0.5$, which would be observed as a pinched core.

We assume that filaments in the same region of a molecular cloud are embedded in a constant background pressure. In this case, filaments with different line-masses will vary substantially in central density and therefore also in the perturbation growth time as it goes as $\tau_{\text{dom}} \sim 1/\sqrt{\rho_c}$. This fact is illustrated in [Figure 3](#) where we show the same evolution of the core to filament radius ratio as in [Figure 1](#) under the assumption that the cores grow on the dominant timescale now for a constant external pressure of $p_{\text{ext}}/k_B = 10^5 \text{ K cm}^{-3}$. Consequently the central density varies from $\rho_c \sim 10^4 \text{ cm}^{-3}$ for low line-masses to $\rho_c \sim 10^6 \text{ cm}^{-3}$ for high line-masses. There is an interesting dichotomy visible in the state of evolution of the cores. High line-mass filaments forming pinched cores evolve much faster than low line-mass filaments which form broad cores. This implies that, as long as there is not much spread in initial perturbation strength in filaments, a region will most likely only contain one population of cores. Either there are mainly pinched cores and broad cores will not have had enough time to grow or there are mainly broad cores and their high line-mass counterparts have already collapsed away and formed stars. Varying the value of the external pressure only shifts the evolutionary tracks in [Figure 3](#) (higher external pressure imply larger central densities and thus faster growth times) and does not change the general behavior.

4 DISCUSSION AND CONCLUSIONS

The gravitational instability model has several shortcomings. The main assumption is that filaments are very idealized cylindrical entities where the mean initial line-mass does not vary much along its length. Moreover, the filament profile requires a certain timescale to adjust to density changes. If the local line-mass varies faster than the radius can adjust, a broad core could be embedded in a filament with a line-mass larger than half the critical value. There are two processes which can lead to a major change in local line-mass on a short timescale. On the one hand, mass accretion increases the overall line-mass. Observed rates are estimated to be on the order of $10 - 100 M_{\odot} \text{ pc}^{-1} \text{ Myr}^{-1}$ (Palmeirim et al. 2013). On the other hand, a filament will longitudinally contract due to self-gravity. In addition, the rapid formation of two cores at the ends of the filament seems to be a typical outcome of the edge-effect (Burkert & Hartmann 2004).

A different equation of state or additional physical contribute to the radial stability and can change the morphology of cores. Observed radial density profiles are better matched by polytropic indices lower than one (Toci & Galli 2015). As long as there is a maximum radius in dependence of the line-mass we still expect a dichotomy in morphology but with the division not necessarily at half the critical line-mass.

Observationally, it is important to not only include the dense gas in order to reliably measure both filament and core radius. As the density of the outer filament gas is lower than the core gas, the filament radius has to be determined with a tracer of low gas density. If only the dense gas is observed, e.g. N_2H^+ , even cores which are nominally pinched can appear broader than the dense gas in the rest of in filament.

Moreover, projection effects can reduce the length of a filament and thus increase the apparent line-mass by a substantial factor. This effect is limited by the fact that higher inclined filaments will not resemble a filamentary structure.

Additionally, more cores are observed which are thinner than the average widths of star-forming filaments (Palmeirim et al. 2013; Marsh et al. 2014; Roy et al. 2014), indicating that most filaments have high line-masses. Nevertheless, higher number statistics on the local ratio of core-to-filament radius are desirable in order to estimate line-masses. All in all, our model allows for the following predictions:

- The morphology of cores embedded in filaments is set by the initial line-mass. Filaments with an initial line-mass below half the critical value will develop broad cores. Filaments with an initial line-mass above half the critical value will develop pinched cores.
- For filaments which are embedded in the same constant background pressure, the perturbation growth times for low and high line-masses are drastically different. If all filaments start with similar perturbation strengths we expect only one population of cores to be present, only pinched cores at early times and broad cores at late times.
- Using the FWHM to determine the radius underestimates the extent of high density regions of the filament and thus underestimates the ratio of core to filament radius.
- The phase where the radius of pinched cores is significantly different from the overall filament radius is very short and indicates an imminent collapse due to loss of hydrostatic equilibrium.

ACKNOWLEDGEMENTS

We thank the anonymous referee for the valuable input that greatly increased the quality of the paper. AB, MG and SH are supported by the priority programme 1573 "Physics of the Interstellar Medium" of the German Science Foundation and the Cluster of Excellence "Origin and Structure of the Universe". The simulations were run using resources of the Leibniz Rechenzentrum (LRZ, Munich; linux cluster Cool-MUC2).

REFERENCES

- André P., et al., 2010, *A&A*, **518**, L102
 André P., Di Francesco J., Ward-Thompson D., Inutsuka S.-I., Pudritz R. E., Pineda J. E., 2014, *Protostars and Planets VI*, pp 27–51
 Arzoumanian D., et al., 2011, *A&A*, **529**, L6
 Arzoumanian D., André P., Peretto N., Könyves V., 2013, *A&A*, **553**, A119
 Benson P. J., Myers P. C., 1989, *ApJS*, **71**, 89
 Bonnor W. B., 1956, *MNRAS*, **116**, 351
 Burkert A., Hartmann L., 2004, *ApJ*, **616**, 288
 Ebert R., 1955, *Z. Astrophys.*, **37**, 217
 Federrath C., 2016, *MNRAS*, **457**, 375
 Fiege J. D., Pudritz R. E., 2000, *MNRAS*, **311**, 105
 Fischera J., Martin P. G., 2012, *A&A*, **542**, A77
 Gehman C. S., Adams F. C., Fatuzzo M., Watkins R., 1996a, *ApJ*, **457**, 718
 Gehman C. S., Adams F. C., Watkins R., 1996b, *ApJ*, **472**, 673
 Hacar A., Tafalla M., 2011, *A&A*, **533**, A34
 Hacar A., Tafalla M., Kauffmann J., Kovács A., 2013, *A&A*, **554**, A55
 Heigl S., Burkert A., Hacar A., 2016, *MNRAS*, **463**, 4301
 Hosseinirad M., Naficy K., Abbassi S., Roshan M., 2017, *MNRAS*, **465**, 1645
 Inutsuka S.-i., Miyama S. M., 1997, *ApJ*, **480**, 681
 Kirk J. M., et al., 2013, *MNRAS*, **432**, 1424
 Klessen R. S., Burkert A., Bate M. R., 1998, *ApJ*, **501**, L205
 Klessen R. S., Ballesteros-Paredes J., Vázquez-Semadeni E., Durán-Rojas C., 2005, *ApJ*, **620**, 786
 Könyves V., et al., 2010, *A&A*, **518**, L106
 Larson R. B., 1985, *MNRAS*, **214**, 379
 Marsh K. A., et al., 2014, *MNRAS*, **439**, 3683
 McKee C. F., Ostriker E. C., 2007, *ARA&A*, **45**, 565
 Men'shchikov A., et al., 2010, *A&A*, **518**, L103
 Myers P. C., 2009, *ApJ*, **700**, 1609
 Nagasawa M., 1987, *Progress of Theoretical Physics*, **77**, 635
 Ostriker J., 1964, *ApJ*, **140**, 1056
 Padoan P., Juvela M., Goodman A. A., Nordlund Å., 2001, *ApJ*, **553**, 227
 Palmeirim P., et al., 2013, *A&A*, **550**, A38
 Roy A., et al., 2014, *A&A*, **562**, A138
 Schneider S., Elmegreen B. G., 1979, *ApJS*, **41**, 87
 Shu F. H., Adams F. C., Lizano S., 1987, *ARA&A*, **25**, 23
 Stodólkiewicz J. S., 1963, *Acta Astron.*, **13**, 30
 Tafalla M., Hacar A., 2015, *A&A*, **574**, A104
 Teyssier R., 2002, *A&A*, **385**, 337
 Toci C., Galli D., 2015, *MNRAS*, **446**, 2110
 Ward-Thompson D., et al., 2010, *A&A*, **518**, L92

This paper has been typeset from a $\text{\TeX}/\text{\LaTeX}$ file prepared by the author.